Journal of Alloys and Compounds 509 (2011) 7337–7343

Contents lists available at ScienceDirect

Journal of Alloys and Compounds

journal homepage: www.elsevier.com/locate/jallcom

Growth and characterization of chemical bath deposited $Cd_{1-x}Zn_xS$ thin films

R. Mariappan[a], M. Ragavendar[b], V. Ponnuswamy[a,*]

[a] Department of Physics, Sri Ramakrishna Mission Vidyalaya College of Arts and Science, Coimbatore 641020, India
[b] Department of Physics, RVS College of Engineering and Technology, Coimbatore 641 042, India

ARTICLE INFO

Article history:
Received 17 August 2010
Received in revised form 11 April 2011
Accepted 16 April 2011
Available online 23 April 2011

Keywords:
Chemical bath deposition
$Cd_{1-x}Zn_xS$ thin films
XRD
SEM
Optical studies

ABSTRACT

$Cd_{1-x}Zn_xS$ ($0 \le x \le 1$) thin films have been deposited by chemical bath deposition method on glass substrates from aqueous solution containing cadmium acetate, zinc acetate and thiourea at 80 ± 5 °C and after annealed at 350 °C. The structural, morphological, compositional and optical properties of the deposited $Cd_{1-x}Zn_xS$ thin films have been studied by X-ray diffractometer, scanning electron microscopy (SEM), energy dispersive X-ray analysis (EDX), photoluminescence (PL) and UV–vis spectrophotometer, respectively. X-ray diffraction analysis shows that for $x < 0.8$, the crystal structure of $Cd_{1-x}Zn_xS$ thin films was hexagonal structure. For $x > 0.6$, however, the $Cd_{1-x}Zn_xS$ films were grown with cubic structure. Annealing the samples at 350 °C in air for 45 min resulted in increase in intensity as well as a shift towards lower scattering angles. The parameters such as crystallite size, strain, dislocation density and texture coefficient are calculated from X-ray diffraction studies. SEM studies reveal the formation of $Cd_{1-x}Zn_xS$ films with uniformly distributed grains over the entire surface of the substrate. The EDX analysis shows the content of atomic percentage. Optical method was used to determine the band gap of the films. The photoluminescence spectra of films have been studied and the results are discussed.

1. Introduction

$Cd_{1-x}Zn_xS$ thin films have been widely used as a band gap window material in heterojunction solar cells [1–5] and photoconductive devices [6]. In solar cells cadmium sulfide (CdS), with room temperature band gap energy of 2.3 eV is used as an n-type direct gap semiconductor. A highly efficient luminescent material zinc sulfide (ZnS) is a semiconductor with a large band gap. Partial substitution of Zn for Cd mole ratio increases the optical window of the heterojunction solar cells [7]. Moreover, in heterojunction solar cells using $CuGaSe_2$, the use of $Cd_{1-x}Zn_xS$ instead of CdS can lead to an increase in photocurrent by providing a match in the electron affinities of the two materials. This hexagonal $Cd_{1-x}Zn_xS$ ternary compound can also be used as a window material for the fabrication of p–n junctions [8]. $Cd_{1-x}Zn_xS$ thin films can be prepared by variety of techniques, such as electrodeposition, spray pyrolysis [9,25–27], co-evaporation [10,28], dip deposition [11,29], solution growth [12,30] and co-precipitation [31]. However, only a few manuscripts on preparation $Cd_{1-x}Zn_xS$ thin film by chemical bath deposition [32,33] are available, despite being one of the most common methods used for the deposition of II–VI compound semiconductor thin films.

In this work, an attempt has been made to study the preparation and characterization of $Cd_{1-x}Zn_xS$ thin films along with structural, optical properties, morphological and compositional analysis of the films. The effects of annealing temperature on the structural, morphological, compositional and optical properties of $Cd_{1-x}Zn_xS$ thin films were studied and the results are reported.

2. Experimental details

Chemical bath deposition technique was adopted for the preparation of $Cd_{1-x}Zn_xS$ thin films. Cadmium acetate, zinc acetate, thiourea, ammonia, hydrazine hydrate the chemicals used for the preparation were analytical reagent grade (99% purity, E-Merck). $Cd_{1-x}Zn_xS$ thin films were produced on glass substrates by the chemical bath deposition technique. 0.1 M cadmium acetate, 0.1 zinc acetate and 0.1 M thiourea were dissolved in 100 ml of de-ionized water and stirred for 10 min using a magnetic stirrer. NH_3 was added slowly from a burette held vertically to the cadmium acetate solution. Initially the solution becomes milk white and on further addition of NH_3 it becomes clear solution. Thiourea solution was slowly added with cadmium acetate solution under gentle stirring condition. NH_3 was again added till the pH value reaches 11. Under gentle stirring zinc acetate solution was added with Cd + S solution and again pH was adjusted to 11 by adding NH_3. With this 2–4 ml of hydrazine hydrate was added for the faster release of ions. The prepared solution was placed on a hot plate and ultrasonically cleaned glass substrates were placed vertically in the solution. Temperature was maintained at 80 ± 5 °C with a PID controlled temperature monitor for 2 h. After 2 h the films were taken out of the solution, rinsed in de-ionized water to remove the loosely bound $Cd_{1-x}Zn_xS$ powder, and dried in air at 120 °C for 3 h to remove moisture from the solution prior to annealing. These films deposited on glass substrates were annealed in air at 350 ± 5 °C. During annealing the color of the film changed from yellow to orange. Films prepared by this method were uniform smooth and reflecting and are well adherent with the substrate. Solutions used for the production of $Cd_{1-x}Zn_xS$ samples are shown in Table 1.

* Corresponding author. Tel.: +91 4222692461; fax: +91 4222693812.
E-mail address: marijpr@gmail.com (V. Ponnuswamy).

0925-8388/$ – see front matter © 2011 Elsevier B.V. All rights reserved.
doi:10.1016/j.jallcom.2011.04.088

Table 1
Solutions used for the production of $Cd_{1-x}Zn_xS$ thin films.

Zinc composition (x)	Cadmium acetate (0.1 M)	Zinc acetate (0.1 M)	Thiourea (0.1 M)
0	100	–	100
0.2	80	20	100
0.4	60	40	100
0.6	40	60	100
0.8	20	80	100
1.0	–	100	100

Aqueous solutions of cadmium acetate, zinc acetate and thiourea were used as the sources of Cd, Zn and S, respectively and the reactions are as follows;

Cadmium acetate dissolves in water and release Cd^{2+} as

$$Cd(CH_3COO)_2 \rightarrow Cd^{2+} + CH_3COO^- \quad (1)$$

Zinc acetate dissolves in water and release Zn^{2+} as

$$Zn(CH_3COO)_2 \rightarrow Zn^{2+} + CH_3COO^- \quad (2)$$

The sulphite ions are released due to decomposition of thiourea in an alkaline medium as,

$$SC(NH_2)_2 + 3OH^- \rightarrow 2NH_3 + CO_3^{2-} + HS^- \quad (3)$$

$$HS^- + OH^- \rightarrow S^{2-} + H_2O \quad (4)$$

and the formation of $Cd_{1-x}Zn_xS$ takes place according to the chemical reaction as,

$$(1-x)Cd^{2+} + xZn^{2+} + S^{2-} \rightarrow Cd_{1-x}Zn_xS + \text{wasteproduct} \quad (5)$$

X-ray diffraction data of the chemical bath deposited $Cd_{1-x}Zn_xS$ samples were recorded with the help of Philips Model PW 1710 diffractometer with CuKα radiation (λ = 0.1542 nm). Surface morphological and compositional analyses were carried out using scanning electron microscope and energy dispersive X-ray analysis setup (EDX) attached with SEM (Philips Model XL 30), respectively. Photoluminescence spectrograph was recorded in "FP-6500 spectro flurometer". Optical spectrum was recorded using a JASCO-V-570 spectrophotometer.

3. Results and discussion

3.1. X-Ray diffraction studies of $Cd_{1-x}Zn_xS$ thin films

X-ray diffraction patterns recorded for the $Cd_{1-x}Zn_xS$ thin films on glass substrates at bath temperature 80 °C, after annealed at 350 °C are shown in Fig. 1a–f. The different peaks in the diffractogram were indexed and the corresponding values of interplanar spacing '*d*' were calculated and compared with the standard values [13,34]. The XRD reveals that for $x <= 0.6$, the crystal structure of $Cd_{1-x}Zn_xS$ thin films is hexagonal crystal structure with X-ray diffraction peaks corresponding to [0 0 2], [1 0 1], [1 1 0], [1 0 3] and [1 1 2] planes. For $x >= 0.8$, however the $Cd_{1-x}Zn_xS$ films were grown with cubic structure with the prominent X-ray diffraction peaks corresponding to [1 1 1], [2 0 0] and [2 2 0] planes. This means that the transition from the hexagonal structure to the cubic form takes between $x <= 0.6$ and $x >= 0.8$. It is observed that the annealing the samples at 350 °C in air for 45 min resulted the diffraction angle of [0 0 2] and [1 0 1], shift towards higher scattering angles with an increase in the zinc compositions (x), which means that [0 0 2] and [1 0 1] lattice constant decreases as shown in Fig. 2c. The grain size parameter was evaluated Debye–Scherrer formula [14]. The strain ε was calculated from the slope of $\beta\cos\theta$ versus $\sin\theta$ [15].

The dislocation density (δ) can be evaluated from Williamson and Smallman's formula,

$$\delta = \frac{1}{D^2}\text{lines/m}^2 \quad (6)$$

The variation of crystallite size and strain with zinc composition (x) for $Cd_{1-x}Zn_xS$ films deposited at bath temperature 80 ± 5 °C, and annealed at 350 °C is shown in Fig. 2a. It is observed from Fig. 2a,

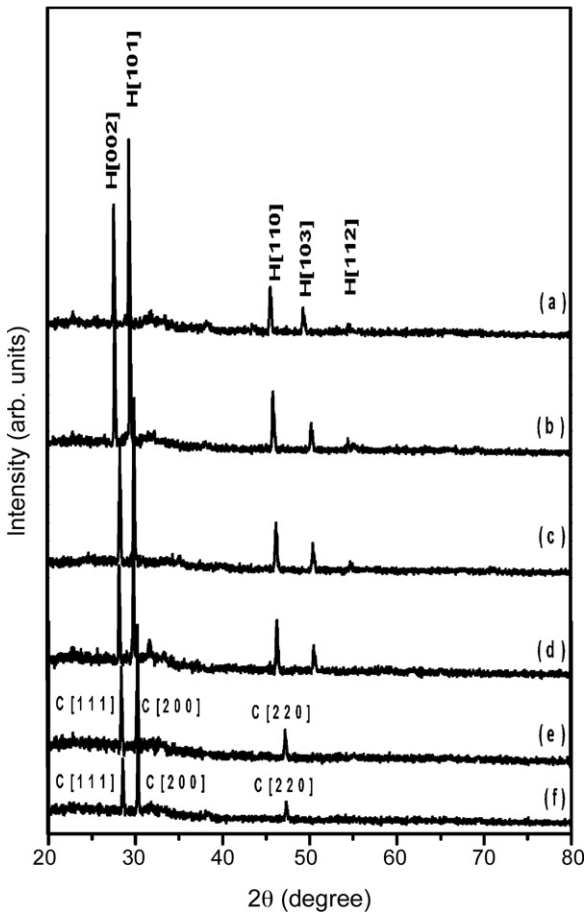

Fig. 1. X-ray diffraction patterns of $Cd_{1-x}Zn_xS$ films deposited at various zinc compositions of: (a) $x = 0$, (b) $x = 0.2$, (c) $x = 0.4$, (d) $x = 0.6$, (e) $x = 0.8$ and (f) $x = 1.0$.

that the crystallite size increases with increasing zinc compositions (x) and found to have maximum value of crystallite size and minimum value of strain. Fig. 2b represents the variation of dislocation density with zinc composition (x) for $Cd_{1-x}Zn_xS$ thin film. It is observed from that (Fig. 2b) the dislocation density found to decrease while increasing zinc compositions (x). A sharp increase in crystallite size and decrease in strain with increasing zinc compositions (x) are indicated in Fig. 2a. Such a release in strain reduced the variation of interplanar spacing and thus leads to decrease in dislocation density of $Cd_{1-x}Zn_xS$ thin films and minimum values are obtained for films annealed at 350 °C. $Cd_{1-x}Zn_xS$ thin films with lower strain and dislocation density improve the stoichiometry of the films which in turn causes the volumetric expansion of thin films. Crystallinity improvement with deposition potential enhances the concentration and mobility of Zn ion vacancies within the lattice and hence reduces the resistivity of the films. The studies on functional dependency of strain and dislocation density with deposition potential indicate that the strain, dislocation density decrease with zinc compositions (x) whereas the crystallite size increases. Similar functional dependency of crystallite size, strain and dislocation density with quartz tube length for CdSe thin films has been reported earlier [14].

The texture coefficient was calculated using the equation [16],

$$T_c = \frac{I_0(h_i\ k_i\ l_i)}{I_s(h_i\ k_i\ l_i)}\left[\frac{1}{n}\sum_{i=1}^{x}\frac{I_0(h_i\ k_i\ l_i)}{I_s(h_i\ k_i\ l_i)}\right]^{-1} \quad (7)$$

where, I_0 is the observed intensity of $[h_i\ k_i\ l_i]$ plane, I_s is the standard intensity of $[h_i\ k_i\ l_i]$ plane and n is the total number

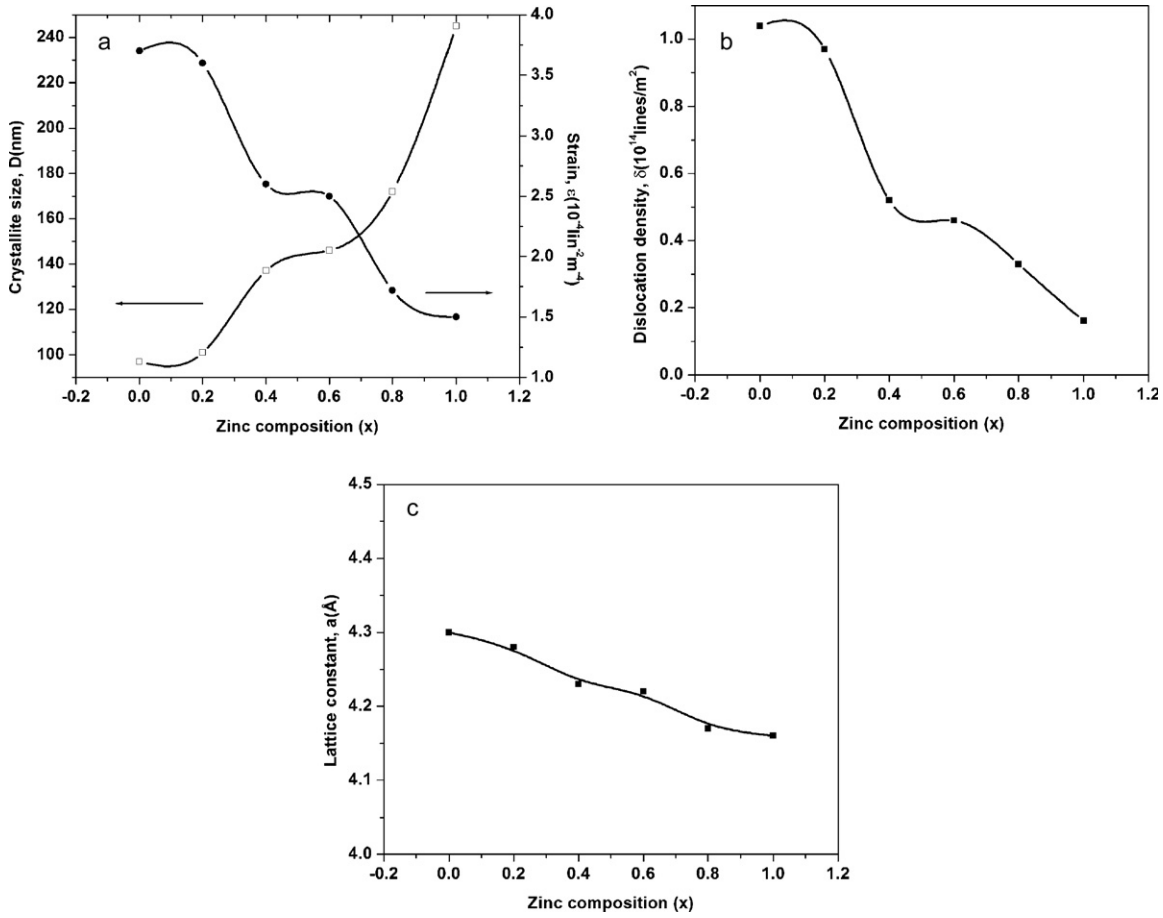

Fig. 2. (a) Variation of crystallite size and strain with zinc composition of $Cd_{1-x}Zn_xS$ thin films. (b) Variation of dislocation density with zinc composition of $Cd_{1-x}Zn_xS$ thin films. (c) Variation of lattice constant with zinc composition of $Cd_{1-x}Zn_xS$ thin films.

of measured reflection. Calculated $T_c[h_i\,k_i\,l_i]$ values give us some important structural information: (i) $T_c[h_i\,k_i\,l_i]$ has to be bigger than 1 to determine the preferential orientation [17], (ii) if $T_c[h_i\,k_i\,l_i]$ approximately 1 for all the $[h_i\,k_i\,l_i]$ planes considered at X-ray diffraction patterns and the films are randomly oriented, (iii) $T_c[h_i\,k_i\,l_i]$ values higher than 1 indicates the abundance of grains in a given $[h_i\,k_i\,l_i]$ direction and (iv) $0 < T_c[h_i\,k_i\,l_i] < 1$ values indicate the lack of grains oriented in that direction [18]. The diffraction angle (2θ), the interplanar spacing (d), miller indices ($h\,k\,l$), crystal system, the observed and standard intensities (I_s and I_0) and texture coefficient (T_s) for all films are listed in Table 2. As can be seen from Table 2, structural parameters were changed depending on the zinc compositions (x). When the T_c $[h_i\,k_i\,l_i]$ values for three peaks given in Table 1 were investigated, it was determined

Table 2
The texture coefficient of $Cd_{1-x}Zn_xS$ thin films.

Zinc composition (x)	2θ	d-Spacing [Å]	($h\,k\,l$) Crystal system	I_0	I_s	T_c
0	28.4738	3.13476	0 0 2	61.03	42	1.986531
	30.2959	2.95025	1 0 1	100.00	100	0.196080
	47.2804	1.92258	1 1 0	23.08	66	0.430632
0.2	28.2570	3.15832	0 0 2	60.24	48	1.994262
	29.8817	2.99019	1 0 1	100.00	100	0.129251
	46.3540	1.95881	1 1 0	20.95	77	0.578074
0.4	28.2570	3.15832	0 0 2	66.05	48	1.994262
	29.8810	2.99010	1 0 1	100.00	100	0.129251
	46.3540	1.95880	1 1 0	31.18	77	0.578000
0.6	28.2110	3.16336	0 0 2	70.99	48	2.124009
	29.8219	2.99605	1 0 1	100.00	100	0.069987
	46.1474	1.96710	1 1 0	23.59	77	0.439925
0.8	27.7412	3.21586	1 1 1	70.99	48	0.312434
	29.5027	3.02774	2 0 0	100.00	100	0.002046
	45.9142	1.97655	2 2 0	23.59	77	0.165822
1.0	28.5416	3.12747	1 1 1	73.93	100	0.256108
	30.2843	2.95435	2 0 0	100	12	0.007751
	47.3105	1.92142	2 2 0	32.17	82	0.105857

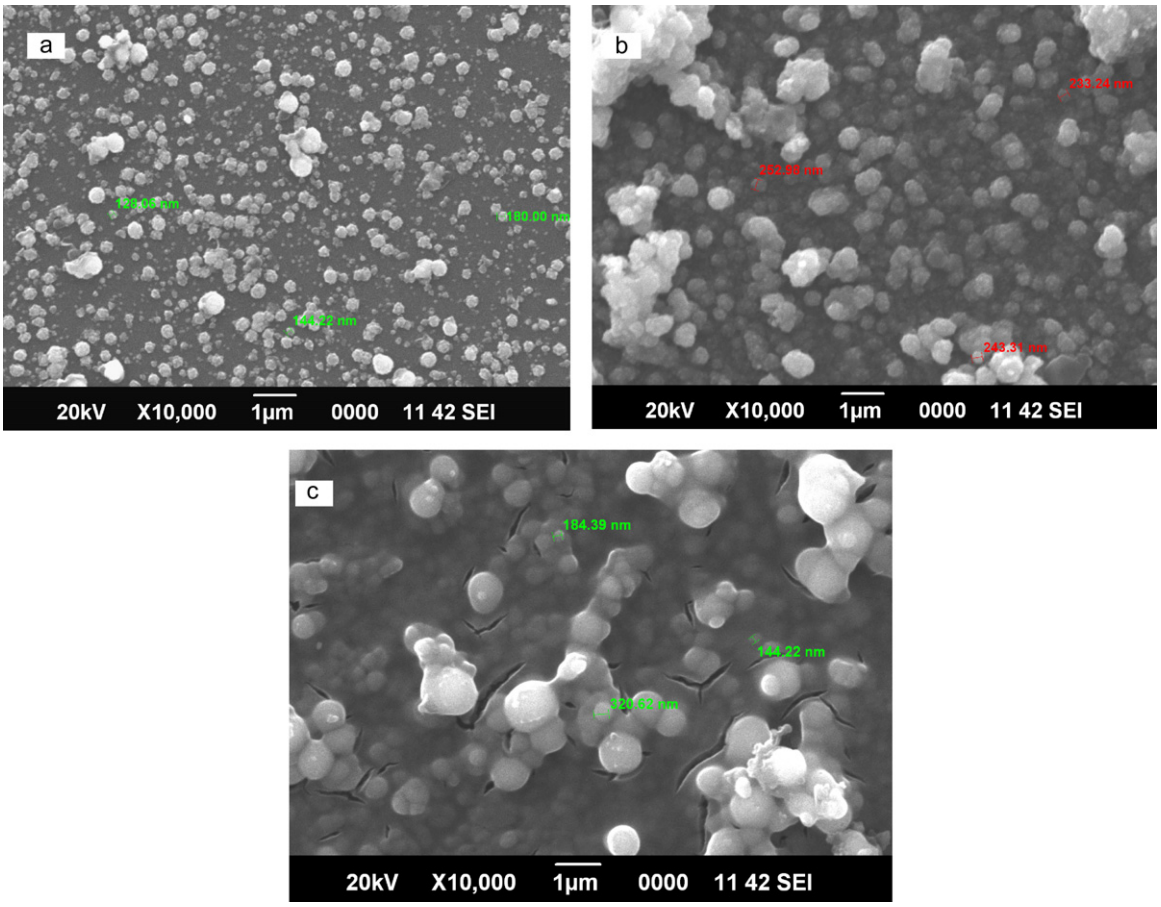

Fig. 3. Typical SEM picture of $Cd_{1-x}Zn_xS$ films deposited at zinc compositions (x) of: (a) $x = 0$, (b) $x = 0.4$, and (c) $x = 1.0$.

that the texture coefficient values of the peaks at $2\theta = 27.5702^\circ$, 28.4738°, 28.2570° and 28.2110° for $x <= 0.6$, $Cd_{1-x}Zn_xS$ films are bigger than one. From these results, the following structural information can be drawn: (i) the preferential orientation of all for $x <= 0.6$, $Cd_{1-x}Zn_xS$ films are through [0 0 2] direction, for $x >= 0.8$, $Cd_{1-x}Zn_xS$ films is through [1 1 1] direction and (iii) $Cd_{1-x}Zn_xS$ films have more grains through [0 0 2] direction, and there is lack of grains oriented through [1 0 1], [1 1 0], [2 0 0] and [2 0 0] directions. The increase in texture coefficient with increase zinc composition (x) indicates an improvement in the crystalline nature of the films.

3.2. Scanning electron microscopy studies of $Cd_{1-x}Zn_xS$ thin films

Fig. 3a–c shows the scanning electron micrographs of $Cd_{1-x}Zn_xS$ films grown at Zinc compositions $x = 0$, 0.4, and 1, respectively. The average particle size is around 250–300 nm in both the micrographs although some of particles in Fig. 3c are much larger. The surface morphology of the films is more or less the same and is similar to that of Fig. 3a as long as the Zn content in the bath $x = 0$, the surface showing smooth and uniform spherical grains without creaks or pinholes and well covered to the glass substrate. As the Zn content is increased to $x = 0.4$, small with uniform grains and well-defined grain boundaries are found in the SEM images. The uniform platelet-like structure thus obtained is shown in Fig. 3b and c. The change in morphology is possibly due to a change in the crystal structure from hexagonal to cubic. The ZnS films annealed at 350 °C show some creaks and pinholes.

3.3. Compositional analyses of $Cd_{1-x}Zn_xS$ thin films

The compositional analysis of the chemical bath deposited $Cd_{1-x}Zn_xS$ thin films annealed at 350 °C were done using energy dispersive X-ray analysis (EDX). The EDX spectra of films annealed at 350 °C are shown in Fig. 4a–c. For $x = 0$, the average atomic percentage of Cd:S was 50.53:49.17 with better stoichiometry in CdS film. In $Cd_{0.6}Zn_{0.4}S$ film the average atomic percentage of Cd:Zn:S was 32.40:20.18:47.42 for $x = 0.4$. Cd content was replaced by Zn content in $Cd_{1-x}Zn_xS$ solid solution films, definitely leading to crystallographic disorder. Cd or Zn interstitial may be created simultaneously. For $x = 1$, ZnS film the average atomic percentage of Zn:S was 44.85:55.15 showing the sample slightly sulfur-rich. The EDX result is consistent with X-ray diffraction analysis of the sample with phase corresponding to CdS, CdZnS and ZnS. Therefore, the films annealed at 350 °C are nearly stoichiometric.

3.4. Photoluminescence studies of $Cd_{1-x}Zn_xS$ thin films

Photoluminescence emission spectra of three $Cd_{1-x}Zn_xS$ ($x = 0$, 0.4, 1.0) thin films annealed at 350 °C are shown in Fig. 5a–c. The spectra have been recorded at room temperature with an excitation wavelength of 361 nm. For $x = 0$, pure CdS films exhibit two broad emission peaks, called green and blue peaks located around 514 and 436 nm, respectively. As the photoluminescence peak energies are less than the energy gap, these bands can be definitely identified with transitions involving donors, acceptors, free electrons and holes [19]. Thus, the well-known green band can be attributed to the recombination between donor and acceptor

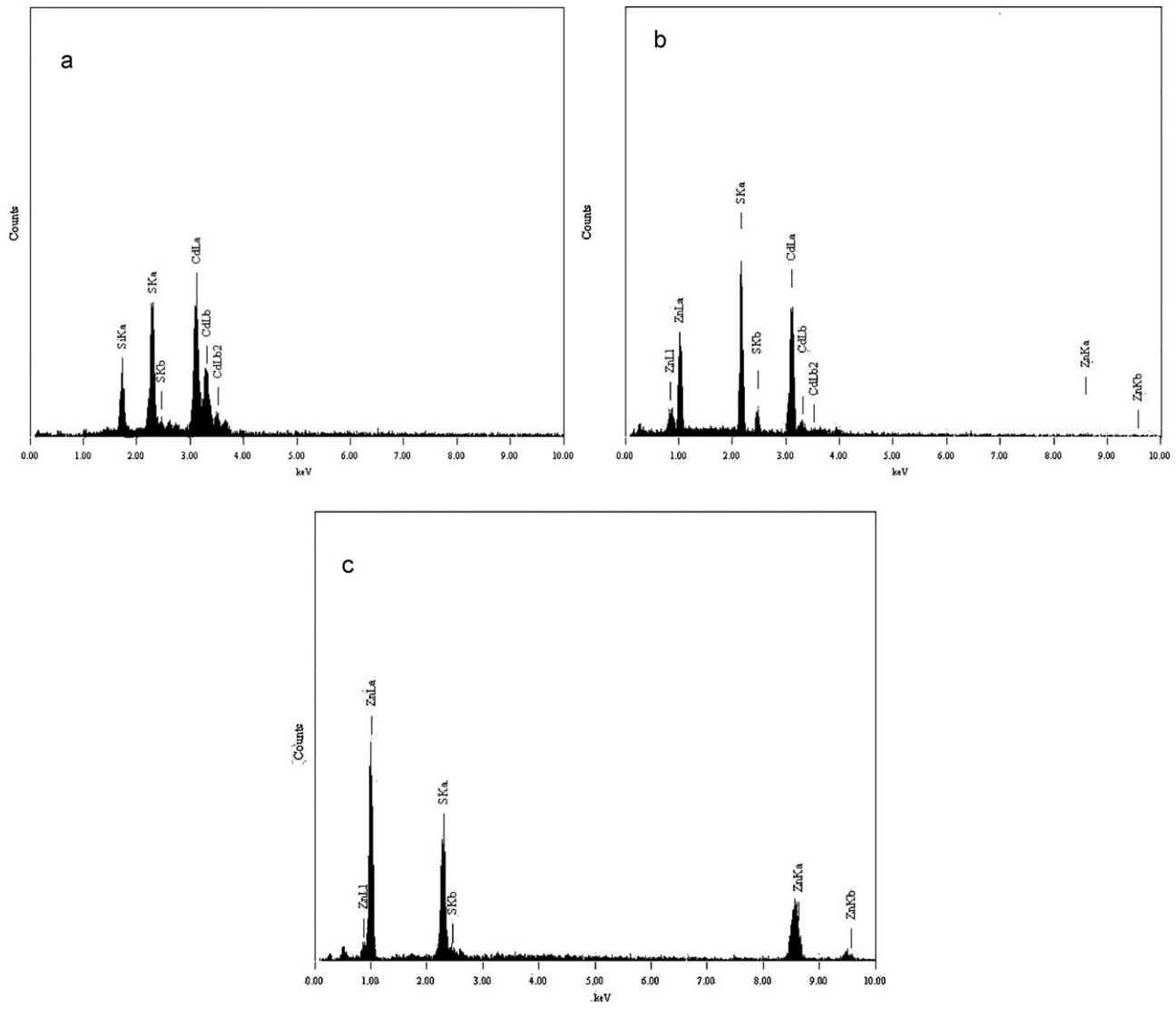

Fig. 4. EDX spectrum of $Cd_{1-x}Zn_xS$ films deposited at zinc compositions x of: (a) $x = 0$, (b) $x = 0.4$, and (c) $x = 1.0$.

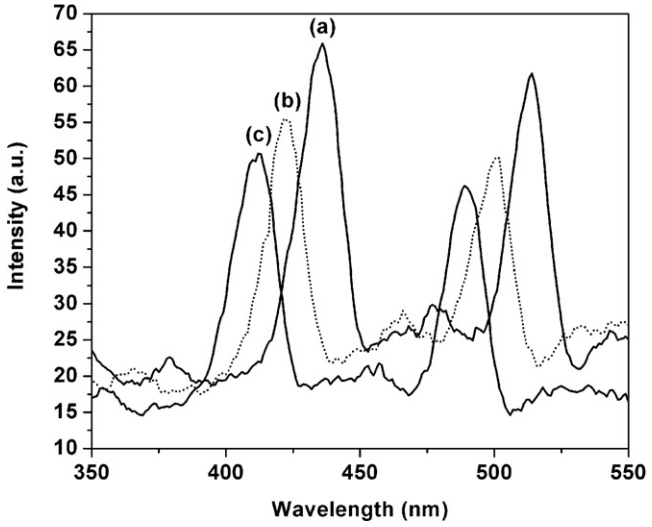

Fig. 5. PL spectrum of $Cd_{1-x}Zn_xS$ films deposited at zinc compositions (x) of: (a) $x = 0$, (b) $x = 0.4$, and (c) $x = 1.0$.

levels originated from surface states i.e., grain boundaries, pinholes, micro deformation, adsorbed oxygen, etc. [19]. In CdS defects consist of cadmium vacancies, sulfur atoms adsorbed on the surface [20]. In the photoluminescence spectra the peak can be attributed to high concentration of defects. The broadening of the peaks can be ascribed to the fact that large crystals tend to harbors more defects than small crystals. These defects may act as non-radiative recombination centres, which band edge recombination [21]. The CdS emission spectra are also found to increase in intensity with decrease in particle size due to the increase in zinc compositions (x). For $x = 0.4$, $Cd_{0.6}Zn_{0.4}S$ films exhibit two emission peaks centred on 500 and 422 nm. The peak position of green and blue slightly shifts towards shorter wavelength and decreases in the peak intensity with zinc compositions (x) increase. The $Cd_{0.6}Zn_{0.4}S$ films present mixed phases either pure CdS or CdZnS [22]. For $x = 1$, ZnS thin films are excited at 361 nm. The plot contains the two peaks centred at 412 and 489 nm. The peak at 489 nm is due to the recombination between the sulfur vacancy related donor and the valence band [23]. The peak position of this emission shifted to shorter wavelength region (412–499 nm) with increase zinc composition (x).

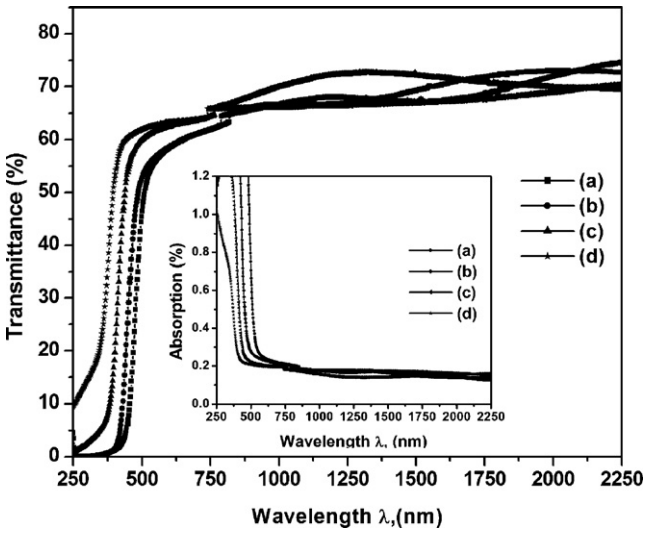

Fig. 6. Transmittance spectra of $Cd_{1-x}Zn_xS$ films (inset Fig. 6: absorption spectra of $Cd_{1-x}Zn_xS$ films) deposited at zinc compositions of: (a) $x = 0$, (b) $x = 0.4$, (c) $x = 0.6$, and (d) $x = 1.0$.

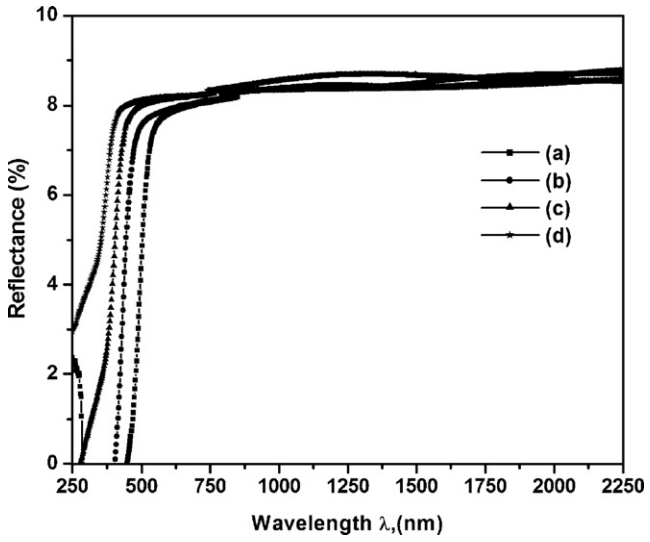

Fig. 7. Reflectance spectra of $Cd_{1-x}Zn_xS$ films deposited at zinc compositions of: (a) $x = 0$, (b) $x = 0.4$, (c) $x = 0.6$, and (d) $x = 1.0$.

3.5. Optical studies of $Cd_{1-x}Zn_xS$ thin films

Optical transmission, absorption and reflectance studies were performed on the chemical bath deposited $Cd_{1-x}Zn_xS$ thin films annealed at 350 °C. Figs. 6 (inset) and 7 represent the transmission, absorption and reflectance curves for $Cd_{1-x}Zn_xS$ films in the zinc compositional range $x = 0$, 0.2, 0.6, and 1. The interference fringes appearing in some of the transmission curves show that the films are of good quality.

The optical constants, refractive index (n) and extinction coefficient (k) of $Cd_{1-x}Zn_xS$ films are calculated from following equation [24].

$$k = \frac{\alpha\lambda}{4\pi} \tag{8}$$

$$n = \frac{1+R}{1-R} + \sqrt{\left[\frac{4R}{(1-R)^2} - k^2\right]} \tag{9}$$

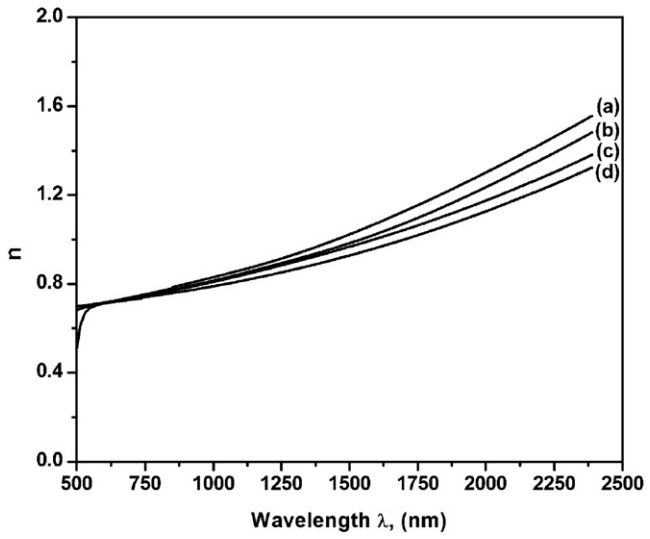

Fig. 8. Refractive index spectra of $Cd_{1-x}Zn_xS$ films deposited at zinc compositions of: (a) $x = 0$, (b) $x = 0.4$, (c) $x = 0.6$, and (d) $x = 1.0$.

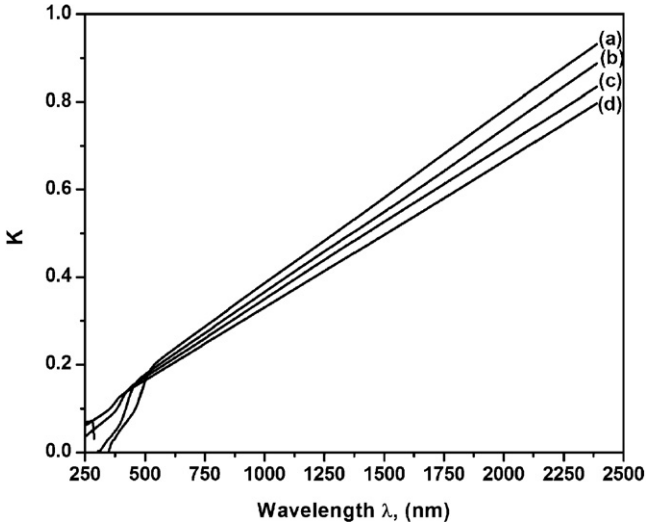

Fig. 9. Extension coefficient spectra of $Cd_{1-x}Zn_xS$ films deposited at zinc compositions of: (a) $x = 0$, (b) $x = 0.4$, (c) $x = 0.6$, and (d) $x = 1.0$.

where 'α'is the absorption coefficient, 'λ' is the wavelength and 'R' is the reflectivity. The refractive index and the extinction coefficient spectra of $Cd_{1-x}Zn_xS$ films are shown in Figs. 8 and 9. It has been observed from the figures that the refractive index and extinction coefficient record trend with wavelength for $Cd_{1-x}Zn_xS$ films. Increase of the refractive index indicates the increase of film density. When the incident light interacts with a material which has large amount of particles, the refraction will be high, and the refractivity of the films will be increased.

The band gaps of the films were calculated using experimentally determined values of α from the following relationship.

$$\alpha = \frac{A(h\nu - E_g)^n}{h\nu} \tag{10}$$

Since $Cd_{1-x}Zn_xS$ is reported as direct band gap material, 'n' is taken as 1/2. So

$$\alpha = \frac{A(h\nu - E_g)^{1/2}}{h\nu} \tag{11}$$

where, A is a constant, 'h' is the Planck constant and 'ν' is the photon frequency. Fig. 10 shows typical plots between $(\alpha h\nu)^2$ versus $h\nu$ for

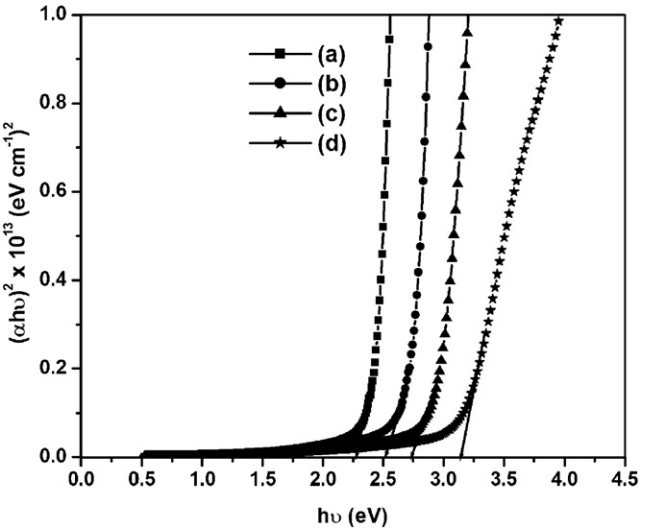

Fig. 10. Band gap of $Cd_{1-x}Zn_xS$ films deposited at zinc compositions of: (a) $x = 0$, (b) $x = 0.4$, (c) $x = 0.6$, and (d) $x = 1.0$.

Table 3
Band gap energy of $Cd_{1-x}Zn_xS$ thin film.

Zinc composition (x)	Film composition	Band gap energy (eV)
0	$Cd_{1.0}Zn_{0.0}S$	2.25
0.4	$Cd_{0.6}Zn_{0.4}S$	2.5
0.6	$Cd_{0.4}Zn_{0.6}S$	2.75
1.0	$Cd_{0.0}Zn_{1.0}S$	3.15

$Cd_{1-x}Zn_xS$ thin films in the compositional range $x = 0$, 0.2, 0.6, and 1. The intercept of the linear plot gives the value of band gap of the samples $Cd_{1-x}Zn_xS$ and given in Table 3.

4. Conclusion

The $Cd_{1-x}Zn_xS$ thin films were deposited on glass substrates at bath temperature 80 °C, using chemical bath deposition technique. X-ray diffraction study shows the formation of polycrystalline $Cd_{1-x}Zn_xS$ films with preferential orientation along [0 0 2] and [1 0 1], shift towards higher scattering angles with an increase in the zinc compositions (x). The structure of the films has been transformed from hexagonal to cubic structure and the surface morphology and grain size also changes with an increase in the zinc compositions (x) which has been confirmed from XRD studies. The crystalline size of the films increases from 97 to 245 nm with the increasing zinc compositions (x). The EDX result is consistent with X-ray diffraction analysis of the sample with phase corresponding to CdS, CdZnS and ZnS. Therefore, the films annealed at 350 °C are nearly stoichiometric. Photoluminescence spectra were taken for $Cd_{1-x}Zn_xS$ thin films to study their emission property. Transmittance spectra are strongly influenced by the deposition conditions. A higher transmission coefficient is observed after a heat treatment. Annealing of the films in air atmosphere gives better physical characteristics to go for solar cell applications. Optical band gap of $Cd_{1-x}Zn_xS$ films varies from 2.3 to 3.4 eV. It is observed that the band gap increases with the zinc composition (x).

References

[1] K.T.R. Reddy, P.J. Reddy, J. Phys. D: Appl. Phys. 25 (1992) 1345–1348.
[2] H.S. Kim, H.B. Im, J.T. Moon, Thin Solid Films 214 (1992) 207–212.
[3] Y.K. Jun, H.B. Im, J. Electrochem. Soc. 135 (1988) 1658–1661.
[4] M. Bulent, Basol, J. Appl. Phys. 55 (1984) 601–603.
[5] K.W. Mitchell, A.L. Fahrenbruch, R.H. Bube, J. Appl. Phys. 48 (1977) 4365–4371.
[6] J. Torres, G. Gordillo, Thin Solid Films 207 (1992) 231–235.
[7] A. Trevor, Chynoweth, H. Richard, J. Appl. Phys. 51 (1980) 1844–1846.
[8] T. Yamaguchi, Y. Yamamoto, T. Tanaka, Y. Demizu, A. Yoshida, Thin Solid Films 281–282 (1996) 375–378.
[9] M. Celalettin Baykul, Nilgun Orhan, Thin Solid Films 518 (2010) 1925–1928.
[10] J.-H. Lee, W.-C. Song, K.-J. Yang, Y.-S. Yoo, Thin Solid Films 416 (2002) 184–189.
[11] S.C. Ray, M.K. Karanjai, Dhruba DasGupta, Thin Solid Films 322 (1998) 117–122.
[12] Y.F. Nicolau, J.C. Menard, J. Cryst. Growth 92 (1988) 128–142.
[13] D.W.G. Ballentyne, B. Ray, Physica 27 (1961) 337–341.
[14] S. Velumani, Sa.K. Narayanadass, D. Mangalaraj, Semicond. Sci. Technol. 13 (1998), 1016-.
[15] S. Thanikaikarasan, T. Mahalingam, K. Sundaram, A. Kathalingam, Y.D. Kim, T. Kim, Vacuum 83 (2009) 1066–1072.
[16] V. Bilgin, S. Kose, F. Atay, I. Akyuz, J. Mater. Sci. 40 (2005) 1909–1915.
[17] N.B. Chaure, R. Jayakrishnan, J.P. Nair, R.K. Pandey, Semicond. Sci. Technol. 12 (1997), 1171-.
[18] R. Romero, D. Leinen, E.A. Dalchiele, J.R. Ramos-Barrado, F. Martin, Thin Solid Films 515 (2006) 1942–1949.
[19] R. Lozada-Morales, O. Zelaya-Angel, G. Torres-Delgado, On the yellow-band emission in CdS films, Appl. Phys. A: Mater. Sci. Processing 73 (2001) 61–65.
[20] X.S. Zhao, J. Schroeder, P.D. Persans, T.G. Bilodeau, Phys. Rev. B 43 (1991) 12580–12589.
[21] N. Pinna, K. Weiss, J. Urban, M.P. Pileni, Triangular CdS Nanocrystals: Structural and Optical Studies 13 (2001) 261–264.
[22] J.M. Dona, J. Herrero, Thin Solid Films 268 (1995) 5–12.
[23] S. Lee, D. Song, D. Kim, J. Lee, S. Kim, I.Y. Park, Y.D. Choi, Mater. Lett. 58 (2004) 342–346.
[24] N. Benramadane, W.A. Murad, R.H. Misho, M. Ziane, Z. Kebbab, Mater. Chem. Phys. 48 (1997) 119–123.
[25] M. Celatettin Baykul, Nilgun Orhan, Thin Solid Films 518 (2010) 1925–1928.
[26] Y. Raviprakash, V. Kasturi, G.K. Bangera, Shivakumar, Curr. Appl. Phys. 10 (2010) 193–198.
[27] Y. Raviprakash, V. Kasturi, G.K. Bangera, Shivakumar, Solar Energy 83 (2009) 1645–1651.
[28] S. stolyarova, M. Weinstein, Y. Nemirovsky, J. Cryst. Growth 310 (2008) 1674–1678.
[29] M. Abdek Rafea, A.A.M. Farag, N. Roushdy, J. Alloys Compd. 485 (2009) 660–666.
[30] S.V. Borse, S.D. Chavhan, Ramphal Sharma, J. Alloys Compd. 436 (2007) 407–414.
[31] C Xing, Y. Zhang, W. Yan, L. Guo, Int. J. Hydrogen Energy 31 (2006) 2018–2024.
[32] T. Premkumar, S. Saravanakumar, K. Sankaranarayanan, Appl. Surf. Sci. 257 (2011) 1923–1927.
[33] W. Xia, J.A. Welt, H. Lin, H.N. Wu, M.H. Ho, C.W. Tang, Solar Energy Mater. Solar Cells 94 (2010) 2113–2118.
[34] W.W. Chen, J.M. Zhang, A.J. Ardell, B. Dunn, Mater. Res. Bull. 23 (1988) 1667–1673.